

New Measurement Methods of Network Robustness and Response Ability via Microarray Data

Chien-Ta Tu, Bor-Sen Chen*

Laboratory of Control and Systems Biology, Department of Electrical Engineering, National Tsing Hua University, Hsinchu, Taiwan

Abstract

“Robustness”, the network ability to maintain systematic performance in the face of intrinsic perturbations, and “response ability”, the network ability to respond to external stimuli or transduce them to downstream regulators, are two important complementary system characteristics that must be considered when discussing biological system performance. However, at present, these features cannot be measured directly for all network components in an experimental procedure. Therefore, we present two novel systematic measurement methods – Network Robustness Measurement (NRM) and Response Ability Measurement (RAM) – to estimate the network robustness and response ability of a gene regulatory network (GRN) or protein-protein interaction network (PPIN) based on the dynamic network model constructed by the corresponding microarray data. We demonstrate the efficiency of NRM and RAM in analyzing GRNs and PPINs, respectively, by considering aging- and cancer-related datasets. When applied to an aging-related GRN, our results indicate that such a network is more robust to intrinsic perturbations in the elderly than in the young, and is therefore less responsive to external stimuli. When applied to a PPIN of fibroblast and HeLa cells, we observe that the network of cancer cells possesses better robustness than that of normal cells. Moreover, the response ability of the PPIN calculated from the cancer cells is lower than that from healthy cells. Accordingly, we propose that generalized NRM and RAM methods represent effective tools for exploring and analyzing different systems-level dynamical properties via microarray data. Making use of such properties can facilitate prediction and application, providing useful information on clinical strategy, drug target selection, and design specifications of synthetic biology from a systems biology perspective.

Citation: Tu C-T, Chen B-S (2013) New Measurement Methods of Network Robustness and Response Ability via Microarray Data. PLoS ONE 8(1): e55230. doi:10.1371/journal.pone.0055230

Editor: Zhi Xie, National Institutes of Health, United States of America

Received: December 12, 2011; **Accepted:** December 28, 2012; **Published:** January 28, 2013

Copyright: © 2013 Tu, Chen. This is an open-access article distributed under the terms of the Creative Commons Attribution License, which permits unrestricted use, distribution, and reproduction in any medium, provided the original author and source are credited.

Funding: This work was supported by the National Science Council of Taiwan with grants NSC 99-2745-E-007-001-ASP and NSC 100-2745-E-007-001-ASP. The funders had no role in study design, data collection and analysis, decision to publish, or preparation of the manuscript.

Competing Interests: The authors have declared that no competing interests exist.

* E-mail: bschen@ee.nthu.edu.tw

Introduction

Biological processes such as development, differentiation, tumorigenesis, and aging are increasingly being described in terms of temporal ordering of highly orchestrated transcriptional programs [1]. Although these processes can be analyzed using high-throughput gene expression microarray data at multiple time points, the computational methods available only identify which genes vary significantly, and how they vary across some or all of the time points measured [2,3]. Despite the technological limitations, system-level properties such as robustness increasingly attracted serious scientific interest in systems biology. Robustness – the ability to maintain continued performance against intrinsic perturbations and uncertainty – has long been recognized as a key property of living systems and has been reviewed extensively elsewhere [4,5]. Moreover, this fundamental and ubiquitously observed system-level phenomenon cannot be understood by focusing on the individual components, even though individual components of a system may or may not be robust themselves.

The term robustness is encountered widely in very different scientific fields, from engineering and control theory to dynamic systems [5] and biology [6,7,8]. It is important to note that robustness describes a relative property, not an absolute one, because no system can maintain stability in all functions when it

encounters a perturbation. In other words, robustness is not immutable. If a system cannot alter itself, it cannot adapt to intrinsic perturbations or changes to its internal environment. Most robust biological systems possess a set of certain mechanisms to achieve this: in particular, both positive and negative feedback control are ubiquitous. Negative feedback, the main mechanism used to achieve a robust response to perturbations, promotes the restoration of an initial condition of a system. Positive feedback amplifies sensitivity to changes and perturbations, a necessary feature for a cell that needs to make decisions robustly [9,10]. Therefore, feedback control is coupled with redundancy to enhance robustness. A signal transduction system is an additional network system that can be considered: it also plays an important role in responding to upstream signals or transducing environmental stimuli to downstream transcription factors in intracellular communication. From the signal energy point of view, the network response ability can be considered as system gain. Nevertheless, there is still no systematic method to measure the response ability of a network system at present.

In the last decade, with advances in experimental techniques, many researchers have utilized high-throughput data from DNA microarrays, yeast two-hybrid assays, co-immunoprecipitation, and ChIP-on-chip to study many kinds of bio-molecular networks. To this end, these kinds of data are often integrated

to construct gene regulatory networks (GRNs) and protein-protein interaction networks (PPINs). These molecular networks have been demonstrated to have great potential for revealing the basic functions and essential mechanisms of various biological phenomena; this is accomplished by understanding biological systems on a system-wide, holistic level rather than in terms of their individual components [11].

Although the concept of robustness tradeoffs has been proposed [12], few studies have quantitatively and systematically calculated the robustness and response ability of a network system. The qualitative notion that a biological system that is highly tolerant to perturbations is robust is largely uncontested; yet, there is no generally accepted approach using microarray data that can analyze robustness quantitatively and systematically from a systems biology perspective. Moreover, in a GRN or PPIN, each component can transduce the effects of external stimuli downstream, but the response ability of the network from the global point of view cannot be experimentally measured for all network components. To solve this problem, we propose estimating the response ability of a GRN or PPIN via microarray data computations. In this study, we present a new measurement method, the Network Robustness Measurement (NRM), to estimate the relative robustness of a GRN or PPIN at different time stages of biological processes and under distinct biological conditions, checking their ability to tolerate intrinsic perturbations and uncertainties based on Lyapunov stability theory. Moreover, we also propose another novel measurement method, the Response Ability Measurement (RAM), to estimate the ability of a network system to respond to and then transduce external stimuli to downstream regulators.

In addition, we illustrate our approaches by applying them to two distinct network systems: a GRN and a PPIN. First, the NRM and RAM are applied to an aging-related GRN constructed via microarray data. We show that a GRN is more robust to intrinsic perturbations in the elderly than in the young, and as such possesses poor response ability to external stimuli. We then applied these methods to PPINs of fibroblast and HeLa cells under oxidative stress conditions. We observe that the PPIN of cancer cells possesses better robustness than that of normal cells under oxidative stress. Moreover, the response ability of the PPIN calculated from the cancer cells is lower than that of the healthy cells. Since “robustness” and “response ability” are two complementary antagonistic characteristics of a network system in the context of system performance (i.e., a more robust system will be less responsive, and vice versa [13]), measurements of these systematic properties could provide verification of the system characteristics of biological networks constructed from microarray data. Measuring the properties of such trade-offs between the robustness and response ability of a network system may provide insight into systemic changes that occur under different biological conditions. These generalized NRM and RAM methods represent effective tools for exploring and analyzing different systems-level dynamical properties. Making use of such properties can facilitate not only predictions and applications in gene therapy and drug target selection from the perspective of systems biology, but also help calibrate design specifications of robust synthetic biological networks for practical applications [14,15,16]. Therefore, the proposed methods may have great potential for analyzing and designing the next generation of synthetic GRNs or PPINs.

Materials and Methods

Since we provide test cases of measuring the robustness and response ability of a GRN and a PPIN in the Results section, here

we will focus on how to construct dynamic system models for a GRN and a PPIN from microarray data and other databases. Then using these dynamic models, we will propose two methods to measure their robustness and response ability.

Constructing a Dynamic Model for a Gene Regulatory Network (GRN)

It is assumed that the network of genes of interest consists of Z genes, and the time-series microarray data used for constructing the GRN contains K time points. In order to take into account the delayed effects of molecular trafficking and cellular signal transduction, the GRN can be represented by the following linear discrete-time dynamic system:

$$X[t+1] = AX[t] + H + n[t]$$

$$A = \begin{bmatrix} \alpha_{1,1} & \alpha_{1,2} & \cdots & \cdots & \alpha_{1,Z} \\ \alpha_{2,1} & \ddots & & & \\ \vdots & & \alpha_{i,j} & & \\ \vdots & & & \ddots & \\ \alpha_{Z,1} & & & & \alpha_{Z,Z} \end{bmatrix}, H = \begin{bmatrix} h_1 \\ h_2 \\ \vdots \\ h_Z \end{bmatrix} \quad (1)$$

where the state vector $X[t] = [x_1[t] x_2[t] \dots x_Z[t]]^T$ stands for the discrete-time mRNA expression levels of total Z genes at times $t = 1 \dots K$. The system matrix A denotes the gene interactions in the gene network: i.e., $\alpha_{i,j}$ denotes the interaction from gene j to gene i when $i \neq j, \forall i, j = 1 \dots Z$; the constant vector H represents the basal level: i.e., h_i denotes the basal level of the i th gene. $n[t]$ denotes the model residue and measurement noise. If the GRN is nonlinear, then the linear gene network in (1) can be considered as the linearized system at the operation point of interest and H will be related to the location of the operation point of linearization: e.g., for a nonlinear gene network $X[t+1] = f(X[t]) + n[t]$ for some nonlinear interaction $f(X)$, the linearized gene network around equilibrium point of interest X_0 can be represented as $X[t+1] = AX[t] + C + \Delta f(X) + n[t]$, where $A = \frac{\partial f(X[t])}{\partial X[t]}|_{X[t]=X_0}$ and $\Delta f(X)$ denotes the high order non-linear term. In this case, $H = C + \Delta f(X)$ represents the basal level of the linearized system at this equilibrium point of interest. A case of a more general, nonlinear GRN will be discussed later.

Remark 1:

The network parameters of system matrix A and basal level H of GRN in (1) are identified by microarray data via recursive least square estimation method [17] in Text S1.

In the following subsections, we would like to measure robustness and response ability of a PPIN for a given biological phenomenon. Therefore, we need to construct the rough PPIN by data mining and then prune it using microarray data to obtain the refined PPIN for the phenomenon.

Constructing the Rough Protein-protein Interaction Network (PPIN)

In order to obtain a PPIN for a biological phenomenon and investigate its network robustness and response ability, we first need to reconstruct the rough PPIN from microarray data and protein-protein interaction (PPI) information: in this case, our data was taken from STRING (Search Tool for the Retrieval of Interacting Genes/Proteins). STRING, a database of known and

predicted protein interactions, comprises direct (physical) and indirect (functional) associations mined from four sources: genomic context, high-throughput experiments, conserved co-expression and previous knowledge. The database currently covers 5,214,234 proteins from 1,133 organisms. As a preliminary measure, we first perform a Bonferroni correction to select those genes with significantly differential expression (the corrected P -value = $0.01/n$, where $n = 25,802$ denotes the number of genes) from microarray data for inclusion in the target pool. Bonferroni correction, one of the strictest and most conservative multiple testing corrections, adjusts the individual P -value for each gene to keep the overall error rate less than or equal to the user-specified P -cutoff value when performing a statistical test on a group of genes [18,19]. Subsequently, this target pool and the PPI database (STRING) are integrated to indicate the possible PPIs between two selected candidates, and the rough PPIN can then be constructed based on the selected candidates in the protein pool and the potential PPIs among them.

Pruning the Rough PPIN via a Dynamic Model

Modern large-scale studies of PPIs permit the development of protein interaction networks, but all large-scale experiments and databases to date have returned high rates of false-positives [20]. Previous evidence has clearly demonstrated that utilizing multiple functional databases not only allows for better identification of PPIs, but also leads to better prediction of the function of unknown proteins [21]. The rough PPIN constructed here comprehensively details the protein interactions possible under all kinds of biological situations and experimental conditions. As such, these interactions must be further narrowed down by microarray data so that they represent only the protein interactions appropriate for the conditions under consideration. Therefore, we use a dynamic PPI model and model order selection method, Akaike Information Criterion (AIC) [22], together to prune the rough PPIN using time series microarray data, deleting false positive PPIs in our PPIN. Here, a dynamic PPI model for a rough PPIN can be represented as follows:

$$\omega_i[t+1] = a_{ii}\omega_i[t] + \sum_{j=1}^Q b_{ij}\omega_j[t] + k_i + v_i[t] \quad (2)$$

where $\omega_i[t]$ denotes the expression profile of the i th target protein $\omega_i[t]$ in the rough PPIN at time point t ; $v_i[t]$ denotes the model residue and measurement noise; a_{ii} denotes the influence of the i th target protein on itself at the next time point; b_{ij} denotes the individual interactive ability of protein j in the rough PPIN with target protein $\omega_i[t]$ when $i \neq j$, $\forall i, j = 1 \dots Q$ and the basal interaction k_i represents unknown PPIs or other influences such as mRNA-protein interactions or protein synthesis. Therefore, the PPIN with dynamic protein interactions in (2) can be represented by

$$W[t+1] = RW[t] + K + V[t]$$

where

$$W[t] = \begin{bmatrix} \omega_1[t] \\ \omega_2[t] \\ \vdots \\ \vdots \\ \omega_Q[t] \end{bmatrix}$$

$$R = \begin{bmatrix} a_{11} & b_{12} & \cdots & b_{1(Q-1)} & b_{1Q} \\ b_{21} & a_{22} & & & b_{2Q} \\ \vdots & & \ddots & & \vdots \\ b_{(Q-1)1} & & & \ddots & b_{(Q-1)Q} \\ b_{Q1} & b_{Q2} & \cdots & b_{Q(Q-1)} & a_{QQ} \end{bmatrix}, \quad (3)$$

$$K = \begin{bmatrix} k_1 \\ k_2 \\ \vdots \\ \vdots \\ k_Q \end{bmatrix}, \quad V[t] = \begin{bmatrix} v_1[t] \\ v_2[t] \\ \vdots \\ \vdots \\ v_Q[t] \end{bmatrix}$$

where R denotes the interactive matrix of the PPIN, K denotes the basal levels of the PPIs, and $V[t]$ denotes the modeling and measurement errors.

Remark 2:

The protein interaction model in (2) can be used to describe any target protein in the rough PPIN. Therefore, the whole PPIN can be described by the protein interaction model described in (3).

In equation (2), $\omega_i[t]$ denotes the expression profile of the i th target protein at time point t , which is estimated from mRNA expression profiles through the following translational sigmoid function [23]:

$$\omega_i[t] = f_i(x_i[t]) = \frac{1}{1 + \exp[-r(x_i[t] - M_i)]} \quad (4)$$

where r denotes the transition rate of the sigmoid function, M_i denotes the mean mRNA expression level of the corresponding protein i , and $x_i[t]$ represents the corresponding mRNA expression profiles of the i -th target gene in the rough PPIN.

Remark 3:

The network parameters R and K of PPIN in (3) are also identified by the recursive least square estimation method [17]. Further a system order detection method, i.e. Akaike Information Criterion (AIC), is employed to detect the number Q of protein interactions in interactive matrix R in (3), i.e. use AIC to prune the false positive protein interactions in R (see Text S2).

Network Robustness Measurement (NRM) of a Dynamic Network System

After constructing the dynamic models of the GRN in (1) and the PPIN in (3) from time series microarray data by the recursive least square estimation method as detailed above, we will measure their network robustness based on these dynamic models. The steady state X_s of the dynamic system in (1) is obtained as:

$$X_s = AX_s + H, \text{ or } X_s = (I - A)^{-1}H \quad (5)$$

To simplify analysis of “robustness” of the steady state (phenotype) of the GRN, the origin of the dynamic system is shifted to the steady state X_s (i.e., $X[t] = \tilde{X}[t] + X_s$), achieving the following shifted dynamic system by subtracting equation (1) from equation (5) [24].

$$\tilde{X}[t+1] = A\tilde{X}[t] \quad (6)$$

Therefore, the robustness of the network’s steady state becomes the robustness of the shifted network in (6) at the origin $\tilde{X}[t] \equiv 0$. In the shifted dynamic system in (6), if the eigenvalues of A are all inside the unit circle $|Z| \leq 1$ in the complex Z domain, then $\tilde{X}[t] \rightarrow 0$, and $X[t] \rightarrow X_s$, or approaches the steady state asymptotically: that is, the phenotype will still be maintained after a small perturbation $\tilde{X}[t]$. Since robustness of the dynamic system in (1) at the steady state X_s is equivalent to robustness of the dynamic system in (6) at the origin $\tilde{X}[t] \equiv 0$, the shifted dynamic system in (6) will simplify the robustness analysis procedure of a network system [24,25].

Remark 4:

The steady state Ws of the PPIN in (3) is obtained as:

$$Ws = RWs + K, \text{ or } Ws = (I - R)^{-1}K$$

The origin of the dynamic PPIN is shifted to the steady state W_s (i.e., $W[t] = \tilde{W}[t] + W_s$), achieving the following shifted dynamic system [24].

$$\tilde{W}[t+1] = R\tilde{W}[t] \quad (7)$$

Therefore, the robustness of the PPIN phenotype becomes the robustness of the above shifted PPIN at the origin $\tilde{W}[t] \equiv 0$. We then use this shifted PPIN in (7) to estimate its robustness and response ability in the same way as the GRN in (6) by following the same network robustness measurement (NRM) and response ability measurement (RAM) methods. Bearing this in mind, we only discuss the NRM and RAM of the GRN in (6). The measurements of NRM and RAM of a PPIN follow the same procedure.

The robustness of the shifted network in (6) is a measure of its ability to tolerate intrinsic molecular-level perturbation [13]. If the linear network system suffers from these kinds of perturbations, whether due to process noise, thermal fluctuations or genetic mutations, the interactive matrix A is perturbed as $A(1 + \eta)$, where η denotes the ratio of intrinsic perturbation, and the corresponding additional system perturbation $\Delta A = \eta A$ [13]. Then the network system with intrinsic perturbation considerations factored in can be represented by:

$$\tilde{X}[t+1] = A(1 + \eta)\tilde{X}[t] \quad (8)$$

A higher η value means more intrinsic perturbations, and the larger the η value that a network can tolerate, the greater robustness the network possesses. Since state-dependent intrinsic

perturbations can influence the stability of a network system, we must further discuss the robustness of the perturbative network system in (8). According to quadratic stability theory [25,26], if the Lyapunov equation of energy function for the perturbative network system in (8) is chosen as $V(\tilde{X}[t]) = \tilde{X}^T[t]P\tilde{X}[t]$ for a positive symmetric matrix $P = P^T > 0$, then the system in (8) is quadratically stable if $\Delta V(\tilde{X}[t]) = V(\tilde{X}[t+1]) - V(\tilde{X}[t]) \leq 0$: that is, if the energy of the GRN is not increased by intrinsic perturbations. Based on this idea, we are able to obtain the following robust stability principle for a GRN of interest that is subject to intrinsic perturbations.

Proposition 1: Suppose a network system suffers from intrinsic perturbations as described in (8). The perturbative network is robustly stable if the following inequality has a positive definite solution $P = P^T > 0$:

$$[A(1 + \eta)]^T P [A(1 + \eta)] \leq P \quad (9)$$

Proof: See Text S3.

Remark 5:

- (i) If a network system is free of intrinsic perturbations as in (6) (i.e., $\eta = 0$), the stable condition is reduced to the following matrix inequality, $A^T P A \leq P$, which has a positive definite solution $P > 0$ [13]. In order to guarantee the stability of a perturbation-free network system, eigenvalues of the system interaction matrix A should be inside the unit circle $|Z| \leq 1$ in the Z complex domain: i.e., $A^T A < 1$. From (9), it can be seen that when η is increased gradually, eigenvalues of system interactive matrix A of the perturbation system in (8) should be nearer the origin of the complex domain Z than those from the perturbation-free system in (6) in order to tolerate more intrinsic perturbation η . Some eigenvalues of system interactive matrix A near the unit circle are more easily perturbed outside the unit circle by intrinsic fluctuations, making the perturbative network system unstable. Therefore, the distance between eigenvalue locations of A to the unit circle represents a measurement of robustness for a linear network system.
- (ii) Based on the above analysis, the robustness η^0 of our network system is the maximum perturbation tolerance allowed by the network, and it can be measured by solving the following constrained optimization:

$$\begin{aligned} \eta^0 &= \max \eta \\ &\text{subject to } P > 0 \text{ and (9)} \end{aligned} \quad (10)$$

i.e., the maximum perturbation ratio η^0 tolerable by the network system while maintaining stability. The constrained optimization problem in (10) can be solved by increasing η until no positive solution $P > 0$ exists in (9): i.e., to the highest possible η without violating the robust stability in (9). A positive definite solution $P > 0$ in (9) can be easily obtained by using the Linear Matrix Inequality (LMI) Toolbox of Matlab.

We can solve the above constrained optimization problem to measure the robustness of the network system simply by increasing η until no positive definite solution $P > 0$ can be found in (9), and then the maximal perturbation η^0 tolerated by the network system represents the robustness under intrinsic perturbations. Hence, we

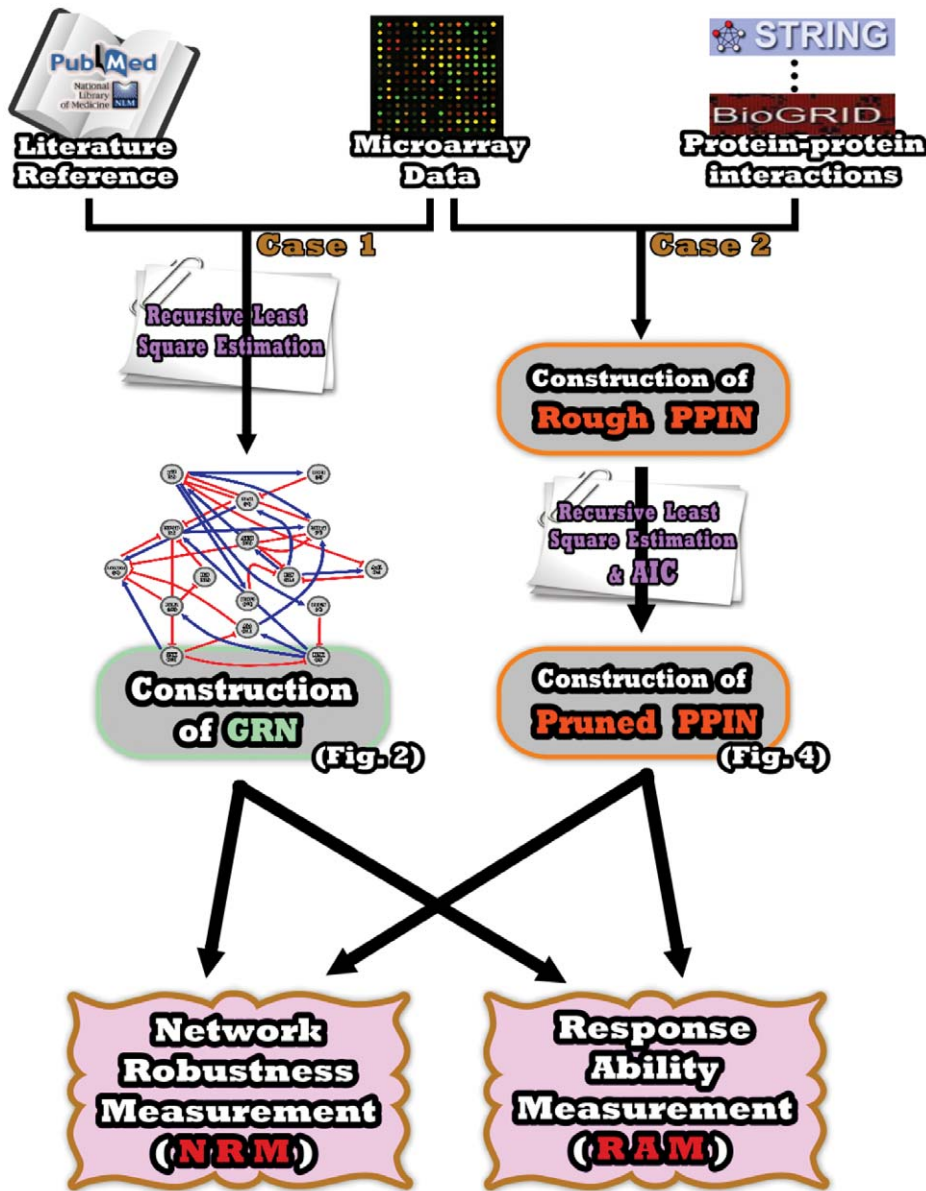


Figure 1. Flowchart of the proposed methods to estimate network robustness and response ability. This flowchart delineates the process used to construct the gene regulatory network (GRN) and protein-protein interaction network (PPIN), and the subsequent estimation of network robustness and response ability by the NRM and RAM methods, respectively. The flow chart on the left represents the Case 1 study analysis of the GRN; the flow chart on the right represents the Case 2 study, where methods are applied to a PPIN. [AIC-Akaike Information Criterion]. doi:10.1371/journal.pone.0055230.g001

are able to obtain the relative robustnesses of network systems we would like to investigate under many different biological circumstances. When comparing η^o for each network, the higher the value of η^o , the greater the robustness estimate for its respective network.

Response Ability Measurement (RAM) of a Dynamic Network System

In this subsection, we turn to how to estimate the response ability of a network system to external stimuli after its robustness has been calculated. Assuming a network system responds to external stimuli $U[t]$, which might include upstream regulatory signals and external signals from factors such as carcinogens,

oxidative stress and ambient pro-inflammatory molecules, the dynamic network (6) is then modified as follows [27].

$$\begin{aligned} \tilde{X}[t+1] &= A\tilde{X}[t] + U[t] \\ Y[t] &= C\tilde{X}[t] \end{aligned} \tag{11}$$

where $U[t] = [u_1[t] u_2[t] \dots u_Z[t]]^T$ represents external stimuli and $Y[t]$ denotes the output signal responses of the network system of interest. For example, if the output signal response of all genes within the network system is analyzed, then $C=I$, an identity matrix. If only the response of the last gene to $U[t]$ is analyzed, the

matrix will be $C = \begin{bmatrix} 0 & \dots & \dots & 0 \\ \vdots & \ddots & & \vdots \\ \vdots & & 0 & 0 \\ 0 & \dots & 0 & 1 \end{bmatrix}$; i.e., all elements of C are zero except for the last element.

In a network system, each component may amplify or attenuate the effect of external stimuli when communicating downstream. The effect of input signals $U[t]$ on output signals $Y[t]$ is less than or equal to a positive value δ , if the following inequality [25,26]:

$$\frac{\sum_{t=0}^{\infty} Y^T[t]Y[t]}{\sum_{t=0}^{\infty} U^T[t]U[t]} \leq \delta^2 \tag{12}$$

or $\sum_{t=0}^{\infty} Y^T[t]Y[t] \leq \delta^2 \sum_{t=0}^{\infty} U^T[t]U[t]$

holds for all possible bounded input signals $U[t] \neq 0$ and $\tilde{X}[0] = 0$. The physical meaning attributable to (12) is that the effect of all possible external stimuli $U[t]$ on $Y[t]$ is less than or equal to δ^2 from the energy point of view: i.e., δ denotes the upper bound of the effect of $U[t]$ on $Y[t]$. If $\tilde{X}[0] \neq 0$, then inequality (12) should be modified as the following [25,26]:

$$\sum_{t=0}^{\infty} Y^T[t]Y[t] \leq \tilde{X}^T[0]P\tilde{X}[0] + \delta^2 \sum_{t=0}^{\infty} U^T[t]U[t] \tag{13}$$

to account for the effect of $\tilde{X}[0]$ on $Y[t]$. δ^o , the smallest upper bound of δ in (12), is called the “network response ability” of the system to all bounded stimulus signals $U[t]$. From δ^o , we obtain a more systematic insight into the ability of a network to respond to external stimuli, which is useful when considering signal transduction or intracellular communication. Via this method, we can measure and compare network response abilities δ^o of various network systems under different biological conditions and states.

Proposition 2: The response of the network system in (11) has an upper bound δ in (12), if there exists a positive definite $P = P^T > 0$ solution to the following linear matrix inequality (LMI) [28]:

$$\begin{bmatrix} A^T P A + C^T C - P & A^T P \\ P A & P - \delta^2 I \end{bmatrix} \leq 0 \tag{14}$$

i.e., if the above LMI holds for some $P > 0$, then the effect of $U[t]$ on $Y[t]$ must be less than or equal to δ : i.e., (12) or (13) hold for the network system in (11).

Proof: See Text S4.

Remark 6:

- (i) The response ability δ^o of a network system to external stimuli can be obtained by minimizing its upper bound δ , achieved by solving the following constrained optimization problem:

$$\delta^o = \min_P \delta \tag{15}$$

subject to $\delta > 0, P > 0$, and (14)

This constrained optimization can be solved by decreasing the upper bound δ in (12) until no $P > 0$ exists in (14) using Matlab LMI toolbox [27].

- (ii) δ^o , the smallest upper bound of δ in (12), is called the network response ability of a network system to external stimuli. If $\delta^o < 1$, it means external stimuli are attenuated (buffered) by the network system; if $\delta^o > 1$, external stimuli are amplified.
- (iii) Since the output/input signal energy ratio (i.e., the response) in (12) or (13) is considered for all possible external stimuli, the measure of network response ability in (14) and (15) is dependent more on system matrix A than on the external stimuli. This is analogous to the way a lowpass filter is dependent more upon the characteristics of the filter than on noise. Therefore, it is possible to measure the network response ability of a network system from its system characteristics without knowledge of what the external stimuli are, with the caveat that these signals must be bounded. The system matrix A can be estimated from time-series microarray data as in the previous subsections. Therefore, employing the Matlab LMI toolbox, we can use (15) to measure network response abilities using microarray data under different specific experimental conditions.

Extension of Network Robustness and Response ability Measurements to Nonlinear Network Systems

Suppose the GRN or PPIN could be constructed by microarray data for the following nonlinear network system:

$$X[t+1] = f(X[t]) \tag{16}$$

Suppose we are interested in the phenomenon around the equilibrium point X_e — i.e., $X_e = f(X_e)$ — and let $\tilde{X}[t] = X[t] - X_e$. Then, we get the shifted nonlinear network system as:

$$\tilde{X}[t+1] = f(\tilde{X}[t] + X_e) - f(X_e) \triangleq \tilde{f}(\tilde{X}[t]) \tag{17}$$

In this system, $\tilde{X}[t] \equiv 0$ is the equilibrium point of interest. Suppose the nonlinear network in (17) could be globally linearized as described in [27] for all $\tilde{X}[t] = X[t] - X_e$ as:

$$\frac{\partial \tilde{f}(\tilde{X}[t])}{\partial \tilde{X}[t]} \Big|_{\tilde{X}[t] \in \Omega} \tag{18}$$

where $\Omega \in \mathbb{R}^{n \times n}$ denotes the system parameter set of these globally linearized systems. Suppose Ω could be described by a list of its vertices via the following convex hull:

$$\Omega \in Co(A_0 A_1 \dots A_m) \tag{19}$$

By the global linearization technique described in [27], all the globally linearized systems in Ω of the nonlinear system in (16) or (17) could be interpolated by the m linear system $\tilde{X}[t+1] = A_i \tilde{X}[t], i = 1, 2, \dots, m$ at the vertices of convex hull of the polytope:

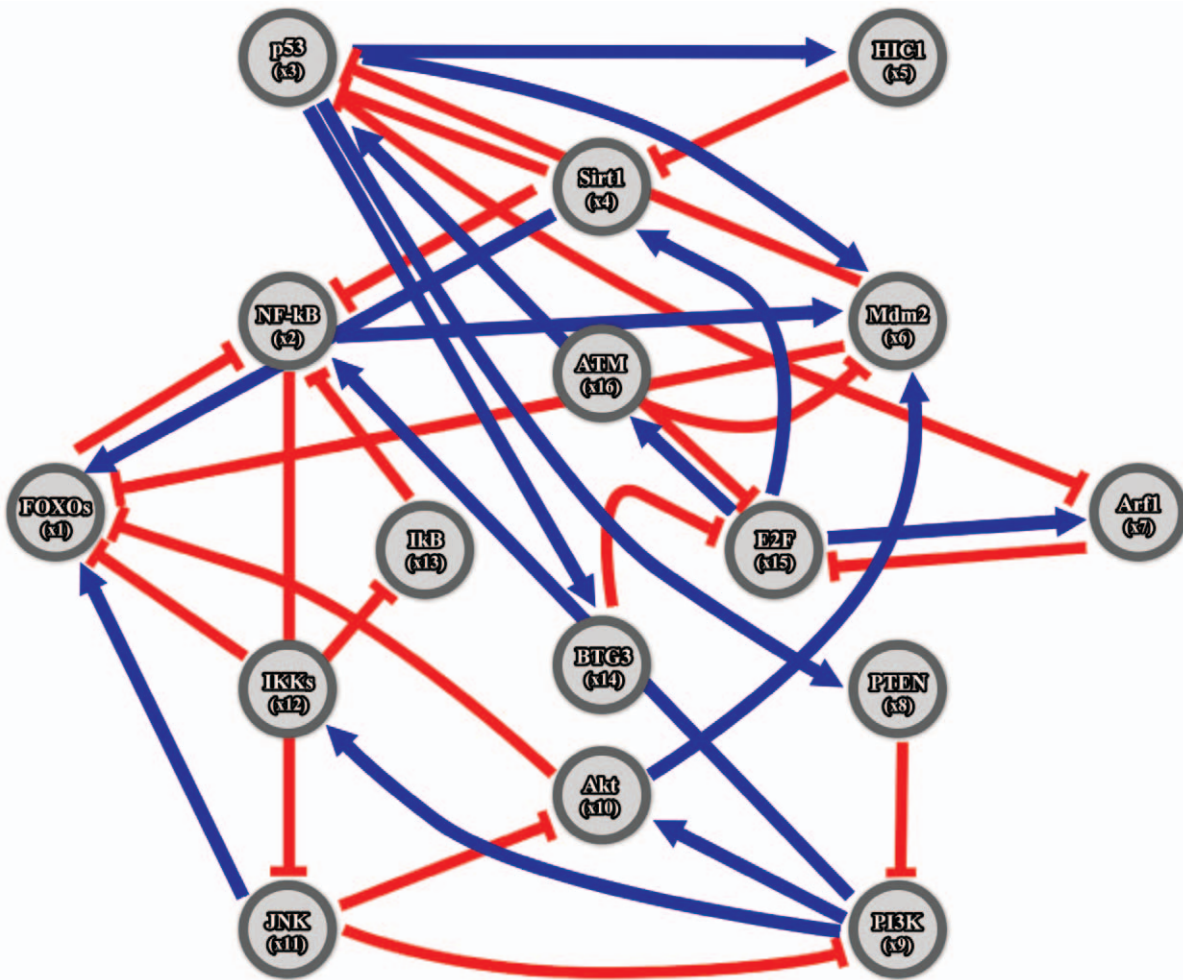


Figure 2. Multiple regulatory loops of a GRN associated with aging-related pathophysiological phenotypes. This network includes the following sixteen genes: FOXOs, NF-κB, p53, SIRT1, HIC1, Mdm2, Arf1, PTEN, PI3K, Akt, JNK, IKKs, IκB, BTG3, E2F1, and ATM. Blue arrows indicate activation; blunt red arrows indicate suppression.
doi:10.1371/journal.pone.0055230.g002

$$\tilde{X}[t+1] = \tilde{f}(\tilde{X}[t]) = \sum_{i=1}^m h_i(\tilde{X}) A_i \tilde{X}[t] \quad (20)$$

where the interpolation functions $h_i(\tilde{X}), i=1, \dots, m$ have the following properties:

$$0 \leq h_i(\tilde{X}) \leq 1, \sum_{i=1}^m h_i(\tilde{X}) = 1 \quad (21)$$

i.e., the trajectory of the nonlinear system in (16) or (17) could be interpolated by the trajectories of m linear systems in (20) via the nonlinear interpolation functions $h_i(\tilde{X}), i=1, \dots, m$

Suppose the nonlinear network system suffers from the following intrinsic perturbations:

$$\tilde{X}[t+1] = \sum_{i=1}^m h_i(\tilde{X}) A_i (1+\eta) \tilde{X}[t] \quad (22)$$

Based on the robust stability principle, we deduce the following.

Proposition 3: Suppose the nonlinear network system suffers from intrinsic perturbations as in (22). The perturbative nonlinear network system is robustly stable if the following LMIs have a positive definition $P = P^T > 0$:

$$[Ai(1+\eta)]^T P [Ai(1+\eta)] \leq P, \text{ for } i=1,2, \dots, m \quad (23)$$

Proof: See Text S5.

The physical meaning of the LMIs in (23) is that the perturbation η is tolerable within all linearized network systems. Therefore, based on the global linearization method, the robustness η^o of the nonlinear network system in (16) can be measured by solving the following constrained optimization:

$$\begin{aligned} \eta^o &= \max \eta \\ \text{subject to } &P > 0 \text{ and LMIs in (23)} \end{aligned} \quad (24)$$

i.e., the maximum perturbation η^o , which is tolerable by all linearized network systems, is a global extension of (15) from a linear network system to a nonlinear network system.

Similarly, if the shifted nonlinear network system with output $Y[t]$ suffers from external stimuli as in:

$$\begin{aligned} \tilde{X}[t+1] &= \tilde{f}(\tilde{X}[t]) + U[t] \\ Y[t] &= C\tilde{X}[t] \end{aligned} \tag{25}$$

then, based on the global linearization technique detailed in [27], the shifted nonlinear network system of (25) with output $Y[t]$ can be represented by the following interpolated system:

$$\begin{aligned} \tilde{X}[t+1] &= \sum_{i=1}^m h_i(\tilde{X}) A_i \tilde{X}[t] + U[t] \\ Y[t] &= C\tilde{X}[t] \end{aligned} \tag{26}$$

Then we get the following result:

Proposition 4: The network response of the nonlinear network system in (26) has an upper bound δ in (12), if there exists a positive definite solution $P = P^T > 0$ to the following LMIs:

$$\begin{bmatrix} A_i^T P A_i + C^T C - P & A_i^T P \\ P A_i & P - \delta^2 I \end{bmatrix} \leq 0, \quad i = 1, 2, \dots, m \tag{27}$$

i.e., if the above LMIs hold for some $P > 0$, then the effect of $U[t]$ on $Y[t]$ must be less than or equal to δ . That is, (12) or (13) holds for the nonlinear network system (25) or (26).

Proof: See Text S6.

Therefore, based on the global linearization method, the network response ability δ^o of the nonlinear network system in (25) or (26) can be measured by solving the following constrained optimization:

$$\begin{aligned} \delta^o &= \min_P \delta \\ &\text{subject to } \delta > 0, P > 0, \text{ and the LMIs in (27)} \end{aligned} \tag{28}$$

Remark 7:

If the nonlinear network system is constructed by the system identification method from microarray or other experimental data, then the network robustness η^o and response ability δ^o can be measured by (24) and (28), respectively. However, to approximate the nonlinear network system via interpolation, these systems must undergo the global linearization in (18) and (19) to find the vertices of the convex hull of the polytope in order to interpolate this linearized system at the vertices (as in the system in (26)). This is generally a very complex task. If we only want to measure the network robustness and response ability of a network system near an equilibrium point (e.g. phenotype), then the measurement methods for network robustness and response ability by (10) and (15) based on a linearized system at its equilibrium point are sufficient. In the following section, we give several practical examples based on linear network systems for measuring the network robustness and response ability of a GRN and PPIN constructed by time-series microarray data.

Results/Discussion

In this paper, we have presented two novel computational methods, Network Robustness Measurement (NRM) and Response Ability Measurement (RAM), which estimate the robust-

ness and response ability of network systems using time-series microarray data. Briefly, the basic methodologies consist of integrating time-series microarray data with either experimental literature or protein-protein interaction information to construct the dynamic system of a gene regulatory network (GRN) or protein-protein interaction network (PPIN). Both of these systems correspond to real phenomena in living organisms and can be used to further evaluate network robustness and response ability (see Figure 1). Details have been described in the preceding Materials & Methods section. These methods are equally applicable to and useful for GRNs and PPINs. In order to demonstrate the potential applications of NRM and RAM for estimating system characteristics exhibited under different biological conditions, we elaborate on the usage of the above methods in two separate cases and explain the analytic results within the following subsection.

Case 1: Estimating the Robustness and Response Ability of a Gene Regulatory Network (GRN) at Different Stages of Life

Aging is an extremely complex and system-level process, and it has attracted much attention in medical research, especially since chronic diseases are quite prevalent in elderly populations. These illnesses may be the result of both gene mutations that lead to intrinsic perturbations and environmental changes that stimulate signaling in the body. In addition, aging may result in reduced responses to environmental stimuli such as carcinogens, oxidative stress, and pro-inflammatory molecules. Therefore, measuring robustness to intrinsic perturbations and response ability to external stimuli of an aging-related GRN could provide key insights into the system-level mechanisms involved in aging.

given GRN, the more robust the GRN is.

Construction of a gene regulatory network associated with aging-related pathophysiological phenotypes. Combing data from several references in the literature, we construct a GRN with multiple regulatory loops that are highly associated with aging-related pathophysiological phenotypes, consisting of the following sixteen genes: FOXOs, NF- κ B, p53, SIRT1, HIC1, Mdm2, Arf1, PTEN, PI3K, Akt, JNK, IKKs, I κ B, BTG3, E2F, and ATM (Figure 2). All genes of interest are critical for regulating cellular functions related to longevity, including detoxification of reactive oxygen species (ROS), cell cycle arrest, repair of damaged DNA, apoptosis, and pro-inflammation, as age increases [29,30]. The GRN can be represented by the linear discrete-time dynamic system shown in Table 1.

In this case, we want to estimate the network robustness and response ability of this GRN, and also to investigate whether they might be altered with increasing age. Furthermore, those altered system characteristics associated with a high incidence of aging-related disease, such as cancer, are prime targets for discussion. The high-throughput microarray data assembled in [31], which details the age-related effects on gene expression in the thymus and spinal cord dissected from male C57BL/6 mice of ages 1, 6, 16, and 24 months, are used as our gene expression profiles. In order to make this data more useful for identifying the system parameters of our dynamic GRN, we first rescale the original gene expression time profiles. For young mice, those aged 17d and 19d are categorized as 3-week-old animals; 40d, 43d, and 44d as 6-week-old animals; 174d, 180d, and 186d as 25-week-old animals; and, 193d and 194d as 28-week-old animals. For aged mice, those aged 476d, 481d, and 485d are categorized as 68-week-old animals; 495d and 498d as 71-week-old animals; 714d and 719d as 102-week-old animals; and, 730d, 733d, and 743d as 105-week-old animals. (All animals had been placed on *ad libitum* diets.) All of the above expression level data are calculated in log2

Table 1. Ordinary differential equations of gene regulatory networks in Figure 2 for sixteen genes associated with aging-related pathophysiological phenotypes.

Gene	Dynamic Equations of Sixteen Genes of Interest
x_1 FOXOs	$x_1[t+1] = \alpha_{1,1}x_1[t] + \alpha_{1,4}x_4[t] + \alpha_{1,6}x_6[t] + \alpha_{1,10}x_{10}[t] + \alpha_{1,11}x_{11}[t] + \alpha_{1,12}x_{12}[t] + h_1$
x_2 NF- κ B	$x_2[t+1] = \alpha_{2,1}x_1[t] + \alpha_{2,2}x_2[t] + \alpha_{2,4}x_4[t] + \alpha_{2,9}x_9[t] + \alpha_{2,13}x_{13}[t] + h_2$
x_3 p53	$x_3[t+1] = \alpha_{3,3}x_3[t] + \alpha_{3,4}x_4[t] + \alpha_{3,6}x_6[t] + \alpha_{3,16}x_{16}[t] + h_3$
x_4 Sirt1	$x_4[t+1] = \alpha_{4,4}x_4[t] + \alpha_{4,5}x_5[t] + \alpha_{4,15}x_{15}[t] + h_4$
x_5 HIC1	$x_5[t+1] = \alpha_{5,3}x_3[t] + \alpha_{5,5}x_5[t] + h_5$
x_6 Mdm2	$x_6[t+1] = \alpha_{6,2}x_2[t] + \alpha_{6,3}x_3[t] + \alpha_{6,6}x_6[t] + \alpha_{6,7}x_7[t] + \alpha_{6,10}x_{10}[t] + \alpha_{6,16}x_{16}[t] + h_6$
x_7 Arf1	$x_7[t+1] = \alpha_{7,3}x_3[t] + \alpha_{7,7}x_7[t] + \alpha_{7,15}x_{15}[t] + h_7$
x_8 PTEN	$x_8[t+1] = \alpha_{8,3}x_3[t] + \alpha_{8,8}x_8[t] + h_8$
x_9 PI3K	$x_9[t+1] = \alpha_{9,8}x_8[t] + \alpha_{9,9}x_9[t] + \alpha_{9,11}x_{11}[t] + h_9$
x_{10} Akt	$x_{10}[t+1] = \alpha_{10,9}x_9[t] + \alpha_{10,10}x_{10}[t] + \alpha_{10,11}x_{11}[t] + h_{10}$
x_{11} JNK	$x_{11}[t+1] = \alpha_{11,2}x_2[t] + \alpha_{11,11}x_{11}[t] + h_{11}$
x_{12} IKKs	$x_{12}[t+1] = \alpha_{12,9}x_9[t] + \alpha_{12,12}x_{12}[t] + h_{12}$
x_{13} I κ B	$x_{13}[t+1] = \alpha_{13,12}x_{12}[t] + \alpha_{13,13}x_{13}[t] + h_{13}$
x_{14} BTG3	$x_{14}[t+1] = \alpha_{13,3}x_3[t] + \alpha_{14,14}x_{14}[t] + h_{14}$
x_{15} E2F	$x_{15}[t+1] = \alpha_{15,7}x_7[t] + \alpha_{15,14}x_{14}[t] + \alpha_{15,15}x_{15}[t] + \alpha_{15,16}x_{16}[t] + h_{15}$
x_{16} ATM	$x_{16}[t+1] = \alpha_{16,15}x_{15}[t] + \alpha_{16,16}x_{16}[t] + h_{16}$

doi:10.1371/journal.pone.0055230.t001

scale, and then the Z-score method is used to normalize the gene array expression data as has been previously described [32].

We construct multiple regulatory loops of a GRN containing sixteen genes (Figure 2) associated with aging-related pathophysiological phenotypes. Using the recursive least square parameter estimation method [17] and the microarray data from the thymus and spinal cord [31], a dynamic model of the sixteen genes within the GRN in equation (1) is constructed (shown in Table 1) with estimated parameters at different stages of life (summarized in Table 2). With equation (1) and Tables 1–2, we calculate sixteen eigenvalues for interactive matrix A at the young and aged stages. The result (Figure 3) shows some eigenvalues of the interactive matrix A clustered together in similar regions near the point $Z = 1$, demonstrating that some modes of the same network will more readily approach some constant steady state than others [12,33].

Estimating network robustness and response ability of GRNs at different stages of life by NRM and RAM methods. It has previously been shown that gene networks associated with aging-related pathophysiological phenotypes suffers from intrinsic perturbations mainly due to noise processes like molecular fluctuation or genetic mutation. The robustness of the GRN is defined as its ability to tolerate intrinsic perturbations and plays a principal role as a fail-safe mechanism during evolutionary processes [12]. Therefore, comparisons of robustness η^o for different GRNs pertaining to young and aged stages may quantitatively describe their relative ability to tolerate these intrinsic perturbations. By using our NRM method, we evaluate the network robustness as shown in Table 3 to represent the maximum intensity of intrinsic perturbations that the network system can tolerate. In other words, the higher the η^o calculated from a

Concerning the RAM, if a GRN also responds to external stimuli $U[t]$, such as upstream signals or biological molecules outside the network, as in equation (11), the network response ability measured should be based on the output/input energy ratio within a time interval as detailed in equation (12). Supposing the

ratio of the effect of input signals $U[t]$ on $Y[t]$ is upper-bounded by a positive value δ , then we can calculate the smallest value δ^o in equation (12) (i.e., the minimum upper bound), and call it the “network response ability” to external stimuli. This method, RAM, is based on system gain theory, and incorporates principles behind the external input signal in system theory perspectives [27]. In general, a GRN with greater robustness always has lower response ability, and vice versa. This is an inherent characteristic of physical systems [27]. The trade-off between robustness and response ability is demonstrably visible in Table 3 and constitutes secondary proof of our proposed method.

Comparing the GRNs of the thymus and spinal cord data between the “young” group and the “aged” group, we show that both tissues evaluated have a higher robustness η^o value in the aged group than the young group. These results are shown in Table 3. The aging-related GRN examined in the first case study is less robust to intrinsic perturbations in the young group than in the aged group. In other words, the GRN at the aged stage can function in spite of the accumulation of DNA damage or genetic mutations accompanying the aging process. In addition, response ability (δ^o) of the GRN calculated from the aged group is lower than that from the young group (Table 3A). In order to tolerate and survive the accumulated intrinsic perturbations (e.g., genetic mutations) associated with the increase in age, the elderly GRN becomes more robust than the young GRN. Therefore, elderly GRNs are less able to respond to external stimuli or transduce them downstream. Hence, the response ability protecting organismal function against external stimuli (e.g., pro-inflammatory molecules) may become worse in the elderly GRN. To confirm the power of the proposed methods, the proposed network robustness and response ability is validated by computer simulation in Figure S1–S3 in Text S7.

In addition, a more robust GRN could harbor more accumulated genetic mutations, which might provide more evolutionary paths to other GRN phenotypes via random drift, and even lead to aging-related diseases like cancers, metabolic disorders, and arthritis [34,35]. On the other hand, the young aging-related

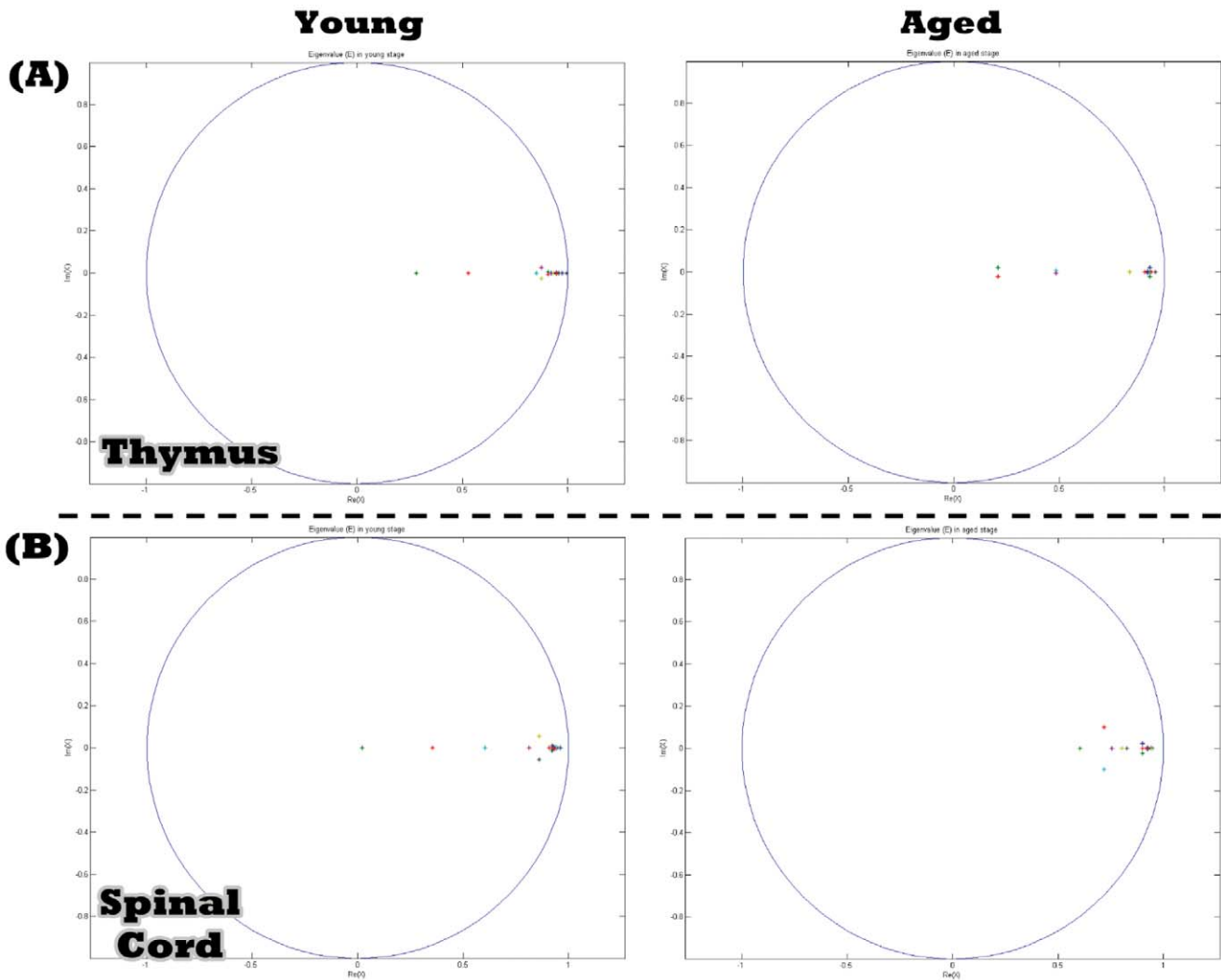


Figure 3. The locations of the sixteen eigenvalues of different tissues at the young and aged stages, respectively. Some eigenvalues of the interactive matrix A for the thymus (A) and spinal cord (B) are located together at similar regions near the unit circle $|Z| = 1$. doi:10.1371/journal.pone.0055230.g003

GRN is less robust, with a greater response to external stimuli. From the above data, we can conclude that the GRNs of the young group more efficiently respond to external stimuli. These values show that while the GRN of the young group is less robust to intrinsic perturbations, external stimuli elicit a strong response from it, suggesting that gene expression may be readily reprogrammed to mediate downstream genes or regulators. This also allows for modulation of gene expression in response to external stimuli such as exposure to oxidative stress, carcinogens, and pro-inflammatory molecules.

Case 2: Estimating the Robustness and Response Ability of a Protein-protein Interaction Network (PPIN) between Normal and Cancer Cells

Robustness, an intrinsic and systematic property of complex biological systems, enables living organisms to maintain their functions in the face of various perturbations to assure their survival [4,12,36]. Moreover, most genes code for sensors, actuators, and the complex regulatory networks that control them, and thus confer robustness to the cell under various challenging circumstances rather than providing merely the basic functionality

required for survival under a single, ideal environment. Normal as well as cancer cells utilize the same processes. At present, although researchers have contended that cancer is a highly robust disease, and clinical observations suggest that inefficiencies in cancer therapy may be due to the according drug resistance, a useful computational method to evaluate the network robustness from microarray data and compare it between cancer and normal cells remains lacking. Therefore, in the second case, the NRM method we have proposed is applied to calculate the PPIN robustness of HeLa cells versus normal fibroblasts under menadione treatment (i.e., exposed to oxidative stress) from corresponding microarray data and protein interaction information. The network response ability is also evaluated and discussed.

Constructing refined PPINs of normal fibroblast cells and HeLa cancer cells under menadione treatment. We use microarray data downloaded from the Gene Expression Omnibus (GEO) database on the NCBI website in this study to investigate the network robustness and response ability of a PPIN in normal cells versus cancer cells under oxidative stress [37]. Normal human diploid lung fibroblasts and HeLa S3 cervical carcinoma cells are treated with 10 μ M menadione bisulfate for 0.5, 1, 3, 4, 6, 8, 12,

Table 2. Estimated parameters of gene regulatory networks in Table 1 with sixteen genes in the thymus (A) and spinal cord (B) at the young and aged stages.

	Parameters of Young Stage				Parameters of Aged Stage				
(A) Thymus	$\alpha_{1,1} = 0.407$	$\alpha_{1,4} = 0.183$	$\alpha_{1,6} = -0.213$	$\alpha_{1,10} = -0.031$	$\alpha_{1,1} = 0.258$	$\alpha_{1,4} = 0.143$	$\alpha_{1,6} = -0.023$	$\alpha_{1,10} = -0.089$	
	$\alpha_{1,11} = 0.060$	$\alpha_{1,12} = -0.408$	$\alpha_{2,1} = 0.099$	$\alpha_{2,2} = 0.964$	$\alpha_{1,11} = 0.033$	$\alpha_{1,12} = -0.401$	$\alpha_{2,1} = 0.186$	$\alpha_{2,2} = 0.525$	
	$\alpha_{2,4} = -0.130$	$\alpha_{2,9} = 0.036$	$\alpha_{2,13} = 0.126$	$\alpha_{3,3} = 0.990$	$\alpha_{2,4} = 0.408$	$\alpha_{2,9} = 0.182$	$\alpha_{2,13} = -0.122$	$\alpha_{3,3} = 1.002$	
	$\alpha_{3,4} = -0.071$	$\alpha_{3,6} = -0.027$	$\alpha_{3,16} = -0.013$	$\alpha_{4,4} = 1.050$	$\alpha_{3,4} = 0.055$	$\alpha_{3,6} = 0.109$	$\alpha_{3,16} = 0.100$	$\alpha_{4,4} = 0.978$	
	$\alpha_{4,5} = 0.026$	$\alpha_{4,15} = 0.004$	$\alpha_{5,3} = -0.001$	$\alpha_{5,5} = 0.998$	$\alpha_{4,5} = 0.036$	$\alpha_{4,15} = 0.04$	$\alpha_{5,3} = 0.019$	$\alpha_{5,5} = 0.978$	
	$\alpha_{6,2} = 0.413$	$\alpha_{6,3} = 0.125$	$\alpha_{6,6} = 0.424$	$\alpha_{6,7} = 0.120$	$\alpha_{6,2} = -0.087$	$\alpha_{6,3} = -0.008$	$\alpha_{6,6} = 0.199$	$\alpha_{6,7} = -0.174$	
	$\alpha_{6,10} = 0.200$	$\alpha_{6,16} = 0.065$	$\alpha_{7,3} = 0.028$	$\alpha_{7,7} = 0.937$	$\alpha_{6,10} = 0.070$	$\alpha_{6,16} = -0.292$	$\alpha_{7,3} = -0.093$	$\alpha_{7,7} = 1.096$	
	$\alpha_{7,15} = -0.006$	$\alpha_{8,3} = 0.008$	$\alpha_{8,8} = 1.106$	$\alpha_{9,8} = -0.011$	$\alpha_{7,15} = -0.107$	$\alpha_{8,3} = 0.05$	$\alpha_{8,8} = 1.001$	$\alpha_{9,8} = -0.027$	
	$\alpha_{9,9} = 0.985$	$\alpha_{9,11} = -0.001$	$\alpha_{10,9} = 0.009$	$\alpha_{10,10} = 1.068$	$\alpha_{9,9} = 0.982$	$\alpha_{9,11} = 0.014$	$\alpha_{10,9} = -0.02$	$\alpha_{10,10} = 0.998$	
	$\alpha_{10,11} = -0.024$	$\alpha_{11,2} = 0.021$	$\alpha_{11,11} = 1.015$	$\alpha_{12,9} = 0.012$	$\alpha_{10,11} = 0.007$	$\alpha_{11,2} = 0.003$	$\alpha_{11,11} = 0.994$	$\alpha_{12,9} = -0.003$	
	$\alpha_{12,12} = 1.019$	$\alpha_{13,12} = 0.009$	$\alpha_{13,13} = 0.998$	$\alpha_{14,3} = -0.003$	$\alpha_{12,12} = 1.028$	$\alpha_{13,12} = 0.029$	$\alpha_{13,13} = 1.009$	$\alpha_{14,3} = -0.092$	
	$\alpha_{14,14} = 1.030$	$\alpha_{15,7} = 0.176$	$\alpha_{15,14} = -0.0799$	$\alpha_{15,15} = 0.964$	$\alpha_{14,14} = 0.965$	$\alpha_{15,7} = 0.366$	$\alpha_{15,14} = 0.253$	$\alpha_{15,15} = 0.454$	
	$\alpha_{15,16} = -0.061$	$\alpha_{16,15} = -0.010$	$\alpha_{16,16} = 1.014$		$\alpha_{15,16} = -0.045$	$\alpha_{16,15} = 0.025$	$\alpha_{16,16} = 0.997$		
	(B) Spinal Cord	$\alpha_{1,1} = 0.388$	$\alpha_{1,4} = 0.082$	$\alpha_{1,6} = 0.004$	$\alpha_{1,10} = -0.161$	$\alpha_{1,1} = 0.886$	$\alpha_{1,4} = 0.044$	$\alpha_{1,6} = 0.085$	$\alpha_{1,10} = 0.043$
		$\alpha_{1,11} = 0.001$	$\alpha_{1,12} = -0.462$	$\alpha_{2,1} = -0.022$	$\alpha_{2,2} = 0.920$	$\alpha_{1,11} = -0.159$	$\alpha_{1,12} = -0.101$	$\alpha_{2,1} = 0.186$	$\alpha_{2,2} = 0.835$
		$\alpha_{2,4} = -0.013$	$\alpha_{2,9} = 0.120$	$\alpha_{2,13} = -0.267$	$\alpha_{3,3} = 0.954$	$\alpha_{2,4} = 0.069$	$\alpha_{2,9} = 0.034$	$\alpha_{2,13} = 0.233$	$\alpha_{3,3} = 0.869$
$\alpha_{3,4} = 0.005$		$\alpha_{3,6} = 0.268$	$\alpha_{3,16} = 0.051$	$\alpha_{4,4} = 0.979$	$\alpha_{3,4} = -0.004$	$\alpha_{3,6} = 0.003$	$\alpha_{3,16} = -0.195$	$\alpha_{4,4} = 0.911$	
$\alpha_{4,5} = -0.043$		$\alpha_{4,15} = 0.129$	$\alpha_{5,3} = 0.080$	$\alpha_{5,5} = 0.974$	$\alpha_{4,5} = 0.242$	$\alpha_{4,15} = -0.364$	$\alpha_{5,3} = -0.044$	$\alpha_{5,5} = 0.998$	
$\alpha_{6,2} = -0.074$		$\alpha_{6,3} = 0.084$	$\alpha_{6,6} = 0.049$	$\alpha_{6,7} = -0.031$	$\alpha_{6,2} = 0.140$	$\alpha_{6,3} = -0.013$	$\alpha_{6,6} = 0.825$	$\alpha_{6,7} = -0.289$	
$\alpha_{6,10} = -0.152$		$\alpha_{6,16} = -0.102$	$\alpha_{7,3} = 0.187$	$\alpha_{7,7} = 1.040$	$\alpha_{6,10} = 0.137$	$\alpha_{6,16} = 0.045$	$\alpha_{7,3} = 0.003$	$\alpha_{7,7} = 0.991$	
$\alpha_{7,15} = -0.157$		$\alpha_{8,3} = 0.037$	$\alpha_{8,8} = 1.009$	$\alpha_{9,8} = -0.006$	$\alpha_{7,15} = -0.007$	$\alpha_{8,3} = -0.019$	$\alpha_{8,8} = 0.998$	$\alpha_{9,8} = -0.091$	
$\alpha_{9,9} = 1.000$		$\alpha_{9,11} = -0.008$	$\alpha_{10,9} = 0.009$	$\alpha_{10,10} = 0.981$	$\alpha_{9,9} = 0.816$	$\alpha_{9,11} = 0.126$	$\alpha_{10,9} = 0.009$	$\alpha_{10,10} = 0.980$	
$\alpha_{10,11} = 0.034$		$\alpha_{11,2} = 0.013$	$\alpha_{11,11} = 1.033$	$\alpha_{12,9} = 0.018$	$\alpha_{10,11} = 0.001$	$\alpha_{11,2} = 0.004$	$\alpha_{11,11} = 0.992$	$\alpha_{12,9} = -0.057$	
$\alpha_{12,12} = 1.023$		$\alpha_{13,12} = -0.002$	$\alpha_{13,13} = 1.015$	$\alpha_{14,3} = 0.596$	$\alpha_{12,12} = 0.972$	$\alpha_{13,12} = 0.007$	$\alpha_{13,13} = 1.011$	$\alpha_{14,3} = -0.011$	
$\alpha_{14,14} = 0.878$		$\alpha_{15,7} = -0.064$	$\alpha_{15,14} = 0.148$	$\alpha_{15,15} = 0.681$	$\alpha_{14,14} = 1.002$	$\alpha_{15,7} = -0.352$	$\alpha_{15,14} = 0.130$	$\alpha_{15,15} = 0.667$	
$\alpha_{15,16} = 0.256$		$\alpha_{16,15} = -0.021$	$\alpha_{16,16} = 1.009$		$\alpha_{15,16} = -0.205$	$\alpha_{16,15} = -0.030$	$\alpha_{16,16} = 1.009$		

doi:10.1371/journal.pone.0055230.t002

24, and 36 hours and 0.5, 1, 2, 4, 8, 12, 24, and 32 hours, respectively. For the oxidative stress condition, the temporal responses at several time points over an interval of 24–36 hours are

Table 3. Estimated network robustness (η^o) and response ability (δ^o).

(A)		Young	Aged
Thymus	η^o	0.2233	0.3852
	δ^o	1.1770	0.9362
Spinal Cord	η^o	0.2360	0.6417
	δ^o	1.1936	0.9073
(B)		Fibroblast	HeLa
Menadione Treatment	η^o	0.1250	1.0016
	δ^o	1.1524	0.6159

Network robustness (η^o) and response ability (δ^o) of the GRN with sixteen genes across different tissues at different stages of life are shown in (A). In addition, the network robustness (η^o) and response ability (δ^o) of PPINs evaluated in normal fibroblast and HeLa cancer cells under menadione treatment are indicated in (B).

doi:10.1371/journal.pone.0055230.t003

measured, allowing stress effects to be observed over an interval longer than a normal cell cycle duration.

As shown in the flowchart in Figure 1, the microarray data are integrated with database information concerning protein interactions as the input for our proposed method (see Materials & Methods). The candidate protein interactions are taken from all experimental conditions in these data to construct the rough PPIN. To proceed further, the corresponding microarray data are used to identify the parameters in equation (8) via the recursive least square estimation method [17], and then to prune down the rough PPINs based on these identified parameters, thus obtaining the refined PPINs of both fibroblast and HeLa cells under menadione treatment via the AIC (shown in Figure 4) [22]. After obtaining the refined PPINs, we can see there are still 161 candidate proteins with 371 interactions in the fibroblast PPIN and 222 candidate proteins with 607 interactions in the HeLa PPIN under oxidative stress conditions. Furthermore, the respective system interactive matrices R of the fibroblast and HeLa cell PPINs can be acquired and then applied to the sequential evaluation of network robustness by equation (10) and response ability by equation (15).

Different network robustness and response ability between the PPINs of normal fibroblasts and HeLa cells both under oxidative stress. We compare the PPINs of fibroblasts and HeLa cells while both are under an oxidative stress insult and show that the PPIN of HeLa cells possesses a higher

Figure 4. Refined protein-protein interaction network. The figure shows the refined PPIN with effective protein interactions under oxidative stress in fibroblast (A) and HeLa cells (B). A dynamic PPI model and model selection method, Akaike Information Criterion (AIC), are used together to prune the rough PPIN using the time series microarray data to delete unrealistic and false positive PPIs in the PPIN. doi:10.1371/journal.pone.0055230.g004

robustness η^0 value than the PPIN of fibroblasts using our NRM method. These results are shown in Table 3B. The PPIN is more robust to such perturbation in the cancer cells than in the normal cells. Moreover, the response ability (δ^0) of the PPIN calculated from the HeLa cells is lower than that from the fibroblasts (Table 3B). Therefore, the PPIN of cancer cells is less efficient in transducing or responding to external stimuli when compared with that of normal cells. The analytic results support previous contentions that cancer cells are more robust than normal cells [38].

Accordingly, compelling evidence has previously suggested that the level of reactive oxygen species (ROS) is higher in many types of cancer cells than in their normal counterparts [39,40,41]. Although a moderate increase in ROS can promote cell proliferation and differentiation, excessive amounts can cause oxidative damage to DNA, protein, and lipids. However, during tumorigenesis or advanced malignant transformation, oncogenic signals can elevate cellular levels of ROS to the extent that numerous genes are altered, accumulating changes via both genetic and epigenetic mechanisms [42,43]. Therefore, cancer cells themselves actively generate high levels of endogenous ROS and are persistently exposed to them, stimulating cell proliferation through redox-sensitive transcription factors and promoting anti-oxidant adaptive mechanisms to minimize oxidative damage [44,45]. Therefore, the intrinsic oxidative stress generated during tumor initiation or malignant transformation may exert selective pressure on the cell population and enrich those capable of stress adaptation: i.e., cancer cells. These cells that survive oxidative stress may have adapted mechanisms to counteract the cytotoxic effects of increased ROS and to promote pathways essential to cellular survival [45]. All of these alterations confer cellular resistance and system robustness to subsequent intrinsic or extrinsic oxidative stress, even at high levels. In clinical cancer therapy, one chemotherapeutic strategy is to elevate excess cellular oxidative stress in order to deplete the antioxidant system and overwhelm the cancer system's ability to neutralize and eliminate such insults, inducing apoptosis and destroying the cancer network system. However, the efficiency of such chemo- or radiotherapy is still unsatisfactory. Moreover, previous evidence has suggested that tumors are highly robust and maintain their proliferative potential against a wide range of anti-cancer therapies. Heterogeneities have been regarded as a vital property of cancer cells because they facilitate robustness through redundancy, and so subsystems killed by chemotherapy can be functionally replaced to ensure tumor proliferation and survival [38]. Hence, the notion of the PPIN of HeLa cells having higher robustness, as evaluated by our proposed NRM method, is consistent with previous contentions and experimental observations. Utilizing microarray data in system-level computations, we have sufficiently demonstrated that cancer cells possess better robustness and less response ability under oxidative stress when compared with normal cells.

References

- Mandel EM, Grosschedl R (2010) Transcription control of early B cell differentiation. *Curr Opin Immunol* 22: 161–167.
- Storey JD, Xiao W, Leek JT, Tompkins RG, Davis RW (2005) Significance analysis of time course microarray experiments. *Proc Natl Acad Sci U S A* 102: 12837–12842.
- Zhu D, Hero AO, Cheng H, Khanna R, Swaroop A (2005) Network constrained clustering for gene microarray data. *Bioinformatics* 21: 4014–4020.
- Stelling J, Sauer U, Szallasi Z, Doyle FJ 3rd, Doyle J (2004) Robustness of cellular functions. *Cell* 118: 675–685.
- Chen BS, Lee TS, Feng JH (1994) A Nonlinear H_∞ control design in robotic systems under parameter perturbation and external disturbance. *International Journal of Control* 59: 439–461.

Conclusions

Our proposed methods, NRM and RAM, consist of multiple analytical steps, from constructing dynamic GRNs and PPINs via microarray data to estimating network robustness and response ability based on their dynamic network systems. However, each individual step can be employed separately, depending on the specific application in question. For example, in the first step we select a set of differentially expressed genes in aging (Case 1) or cancer (Case 2) as our target genes. However, another user could replace this set of genes with other sets of genes of interest to facilitate targeted studies over a wide range of issues. In addition, our proposed methods can evaluate the network robustness and response ability not only for GRNs (Case 1) but also for PPINs (Case 2) depending on the needs of the user. The generalized NRM and RAM methods are effective tools for exploring and analyzing different systems-level dynamical properties. Making use of such network properties can facilitate biomedical predictions and applications, providing useful information for clinical strategy, drug target selection, and design specifications of synthetic biology from the perspective of systems biology [10,14,15,16].

Supporting Information

Text S1 Parameter Identification of a Gene Regulatory Network by Microarray Data. (DOC)

Text S2 Network Parameter Identification of PPIN and Pruning of False Positive Protein Interactions. (DOC)

Text S3 Proof of Proposition 1. (DOC)

Text S4 Proof of Proposition 2. (DOC)

Text S5 Proof of Proposition 3. (DOC)

Text S6 Proof of Proposition 4. (DOC)

Text S7 Computer Simulation of the Proposed Network Robustness and Response Ability Methods. (DOC)

Author Contributions

Carried out model design: CTT. Developed the method: CTT. Provided essential guidance and revised the manuscript: BSC. Conceived and designed the experiments: CTT BSC. Performed the experiments: CTT. Analyzed the data: CTT BSC. Contributed reagents/materials/analysis tools: CTT BSC. Wrote the paper: CTT.

6. Hopfield JJ (1974) Kinetic proofreading: a new mechanism for reducing errors in biosynthetic processes requiring high specificity. *Proc Natl Acad Sci U S A* 71: 4135–4139.
7. Yan J, Magnasco MO, Marko JF (2001) Kinetic proofreading can explain the suppression of supercoiling of circular DNA molecules by type-II topoisomerases. *Phys Rev E Stat Nonlin Soft Matter Phys* 63: 031909.
8. Pastor-Satorras R, Vespignani A (2004) *Evolution and structure of the Internet*: Cambridge University Press.
9. Angeli D, Ferrell JE Jr, Sontag ED (2004) Detection of multistability, bifurcations, and hysteresis in a large class of biological positive-feedback systems. *Proc Natl Acad Sci U S A* 101: 1822–1827.
10. Hasty J, McMillen D, Collins JJ (2002) Engineered gene circuits. *Nature* 420: 224–230.
11. Zhang S, Jin G, Zhang XS, Chen L (2007) Discovering functions and revealing mechanisms at molecular level from biological networks. *Proteomics* 7: 2856–2869.
12. Kitano H (2004) Biological robustness. *Nat Rev Genet* 5: 826–837.
13. Doyle JC, Francis B, Tannenbaum A (1992) *Feedback Control Theory*: Macmillan Publishing Company.
14. Kaern M, Blake WJ, Collins JJ (2003) The engineering of gene regulatory networks. *Annu Rev Biomed Eng* 5: 179–206.
15. Murphy KF, Balazsi G, Collins JJ (2007) Combinatorial promoter design for engineering noisy gene expression. *Proc Natl Acad Sci U S A* 104: 12726–12731.
16. Chen BS, Wu CH (2009) A systematic design method for robust synthetic biology to satisfy design specifications. *BMC Syst Biol* 3: 66.
17. Johansson R (1993) System modeling and identification.
18. Noble WS (2009) How does multiple testing correction work? *Nature Biotechnology* 27: 1135–1137.
19. Bland JM, Altman DG (1995) Multiple Significance Tests - the Bonferroni Method. *British Medical Journal* 310: 170–170.
20. Gandhi TK, Zhong J, Mathivanan S, Karthick L, Chandrika KN, et al. (2006) Analysis of the human protein interactome and comparison with yeast, worm and fly interaction datasets. *Nat Genet* 38: 285–293.
21. Troyanskaya OG (2005) Putting microarrays in a context: integrated analysis of diverse biological data. *Brief Bioinform* 6: 34–43.
22. Akaike H (1974) A new look at the statistical model identification. *Automatic Control, IEEE Transactions on* 19: 716–723.
23. Klipp E, Wierling C, Lehrach H (2005) *Systems Biology in Practice. Concepts, Implementation and Application*. Berlin: Wiley-VCH.
24. Kuo BC, Golnaraghi F (2009) *Automatic Control Systems*: John Wiley & Sons Inc.
25. Chen BS, Zhang W (2004) Stochastic H₂/H_∞ control with state-dependent noise. *IEEE Trans Automatic Control* 49: 45–57.
26. Zhang W, Chen BS (2006) State feedback H_∞ control for a class of nonlinear stochastic systems. *SIAM J on Control and Optimization* 44: 1973–1991.
27. Boyd SP (1994) *Linear matrix inequalities in system and control theory*. Philadelphia: Society for Industrial and Applied Mathematics. ix, 193 p. p.
28. Lin CL, Lai CC, Huang TH (2000) A neural network for linear matrix inequality problems. *IEEE Trans Neural Netw* 11: 1078–1092.
29. Chung HY, Sung B, Jung KJ, Zou Y, Yu BP (2006) The molecular inflammatory process in aging. *Antioxid Redox Signal* 8: 572–581.
30. Judge S, Jang YM, Smith A, Hagen T, Leeuwenburgh C (2005) Age-associated increases in oxidative stress and antioxidant enzyme activities in cardiac interfibrillar mitochondria: implications for the mitochondrial theory of aging. *FASEB J* 19: 419–421.
31. Zahn JM, Poosala S, Owen AB, Ingram DK, Lustig A, et al. (2007) AGEMAP: a gene expression database for aging in mice. *PLoS Genet* 3: e201.
32. Cheadle C, Vawter MP, Freed WJ, Becker KG (2003) Analysis of microarray data using Z score transformation. *J Mol Diagn* 5: 73–81.
33. Tegner J, Yeung MK, Hasty J, Collins JJ (2003) Reverse engineering gene networks: integrating genetic perturbations with dynamical modeling. *Proc Natl Acad Sci U S A* 100: 5944–5949.
34. Lenski RE, Barrick JE, Ofria C (2006) Balancing robustness and evolvability. *PLoS Biol* 4: e428.
35. de Visser JA, Hermisson J, Wagner GP, Ancel Meyers L, Bagheri-Chaichian H, et al. (2003) Perspective: Evolution and detection of genetic robustness. *Evolution* 57: 1959–1972.
36. Csete ME, Doyle JC (2002) Reverse engineering of biological complexity. *Science* 295: 1664–1669.
37. Murray JI, Whitfield ML, Trinklein ND, Myers RM, Brown PO, et al. (2004) Diverse and specific gene expression responses to stresses in cultured human cells. *Mol Biol Cell* 15: 2361–2374.
38. Kitano H (2004) Cancer as a robust system: implications for anticancer therapy. *Nat Rev Cancer* 4: 227–235.
39. Toyokuni S, Okamoto K, Yodoi J, Hiai H (1995) Persistent oxidative stress in cancer. *FEBS Lett* 358: 1–3.
40. Kawanishi S, Hiraku Y, Pinlaor S, Ma N (2006) Oxidative and nitrate DNA damage in animals and patients with inflammatory diseases in relation to inflammation-related carcinogenesis. *Biol Chem* 387: 365–372.
41. Szatrowski TP, Nathan CF (1991) Production of large amounts of hydrogen peroxide by human tumor cells. *Cancer Res* 51: 794–798.
42. Schneider BL, Kulesz-Martin M (2004) Destructive cycles: the role of genomic instability and adaptation in carcinogenesis. *Carcinogenesis* 25: 2033–2044.
43. Wallace DC (2005) The mitochondrial genome in human adaptive radiation and disease: on the road to therapeutics and performance enhancement. *Gene* 354: 169–180.
44. Irmak MB, Ince G, Ozturk M, Cetin-Atalay R (2003) Acquired tolerance of hepatocellular carcinoma cells to selenium deficiency: a selective survival mechanism? *Cancer Res* 63: 6707–6715.
45. Trachootham D, Alexandre J, Huang P (2009) Targeting cancer cells by ROS-mediated mechanisms: a radical therapeutic approach? *Nat Rev Drug Discov* 8: 579–591.